

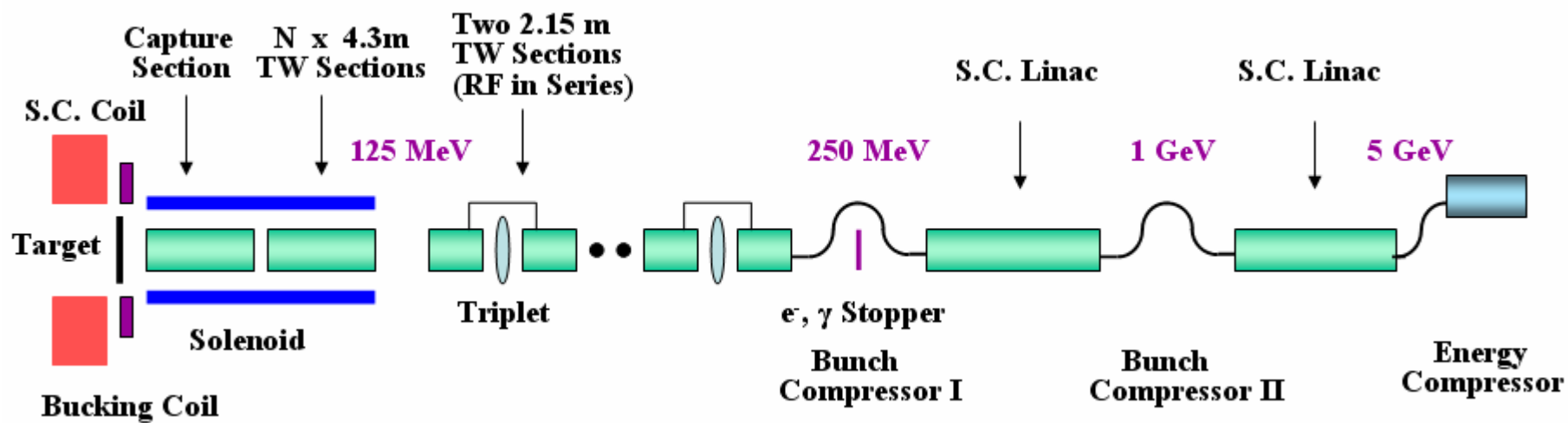


Accelerator and RF System for ILC Positron Source

Second ILC Accelerator Workshop
Snowmass, August 16, 2005

Juwén Wang
SLAC

Schematic Layout of Positron Source



Outline

1. Layout and Introduction.
2. Four Types of Accelerator Structures and Basic Properties.
3. Feasibility Studies
 - Cooling
 - Mode Spacing
 - Cell Phase Difference
 - RF Amplitude and Phase
 - RF Pulse Heating
4. Discussion on Positron Yield – Initial Acceleration and Deceleration.
5. Design of Pre-Accelerator and PARMELA Simulation.
6. Preliminary Plan.

People who also contribute to the studies at SLAC:

C. Adolphsen, G. Bowden, V. Dolgashev, R. Jones, E. Jongewaard,
J. Lewandowski, Z. Li, T. Raubenheimer, R. Miller, C. Pearson.

Introduction

- There have been a lot of studies and papers on design of the accelerator system for ILC positron source. We realize the great challenges in both electrical and mechanical aspects.
- Based on our experiences in normal conducting accelerator structures R&D, we have proposed this preliminary design. We would like to discuss it with our colleagues.



1. Higher gradient (~ 15 MV/m) shorter structures

Single π mode short SW structure or pair of half length sections fed with 3db hybrid for RF reflection cancellation.

- It is simpler and feasible (stabilization) for 11-cavity short SW structure.
- Lower pulse heating.
- Larger iris size (60 mm diameter) with reasonable shunt impedance.
- Efficient cooling design.

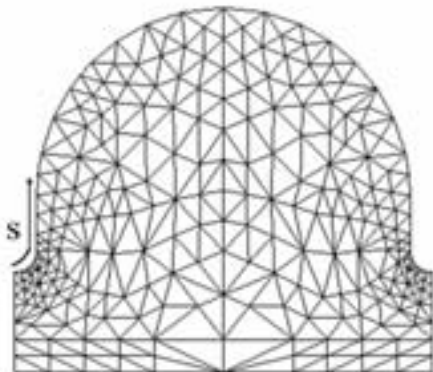
2. Lower gradient (~ 8 MV/m) longer structures

TW constant gradient sections with higher phase advances per cell.

- Using “phase advance per cell” as a knob to optimize the RF efficiency for different length of structure.
- It is simpler and feasible.
- Lower pulse heating.
- Easier cooling design.
- Easier for long solenoids solution.
- Less concern on multipacting and klystron protection from RF power reflection.

3. Four types of structures have been designed.

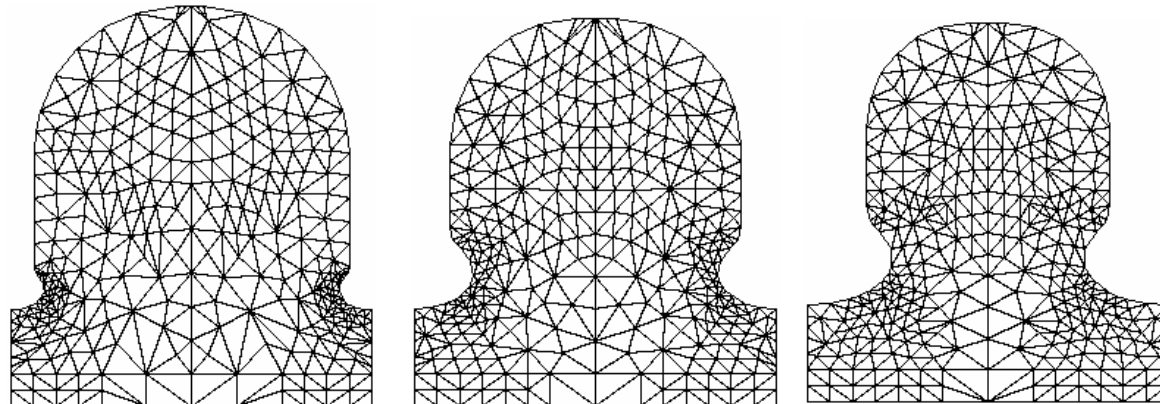
1.27 m long Simple π mode SW Structure



Cell profile

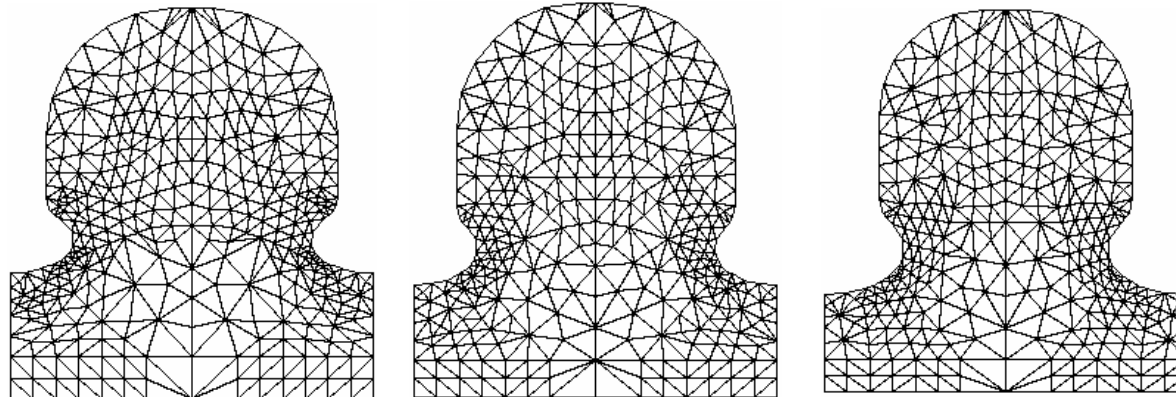
Structure Type	Simple π
Cell Number	11
Aperture 2a	60 mm
Q	29700
Shunt impedance r	34.3 MΩ/m
E_0 (8.6 MW input)	15.2 MV/m

4.3 m long $3\pi/4$ Mode “Regular” TW Structures



Structure Type	TW
Cell Number	50
Aperture 2a	46 mm
Attenuation τ	0.98
Q	24842 - 21676
Group velocity V_g/c	0.62% – 0.14%
Shunt impedance r	48.60 – 39.45 MΩ/m
Filling time T_f	5.3 μs
Power Dissipation	8.2 kW/m
E_0 (10 MW input)	8.5 MV/m

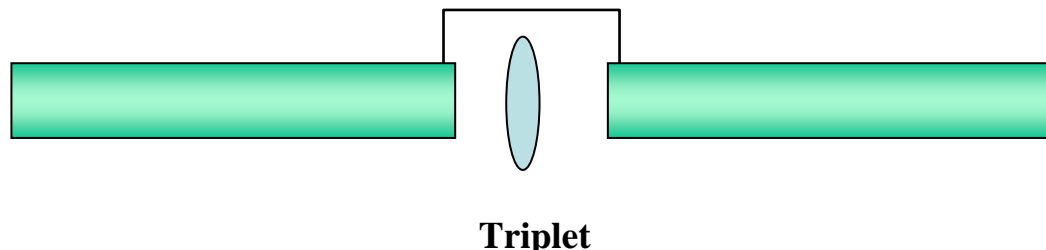
4.3 m long $3\pi/4$ Mode “Special” TW Structures

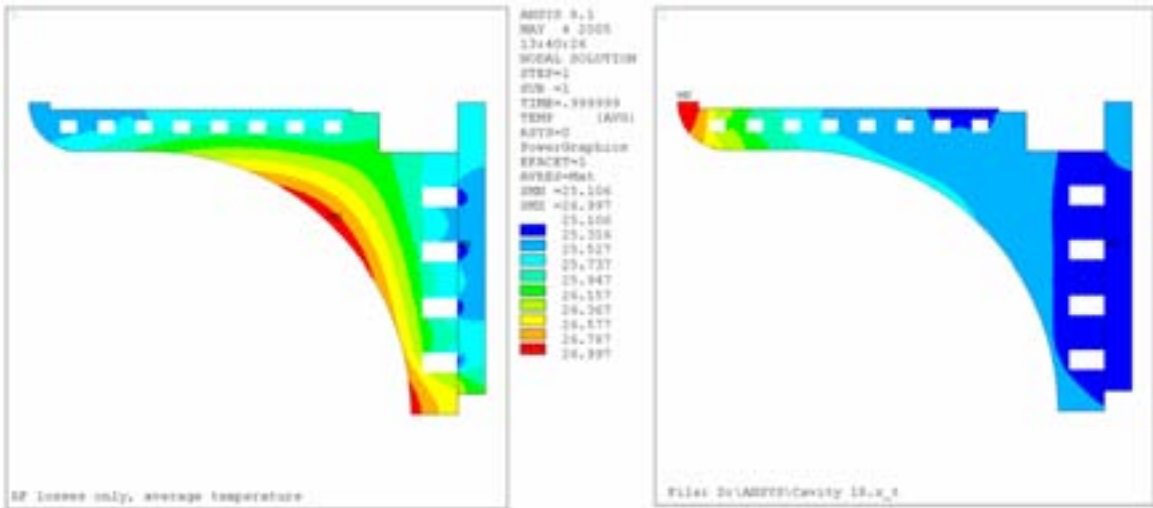
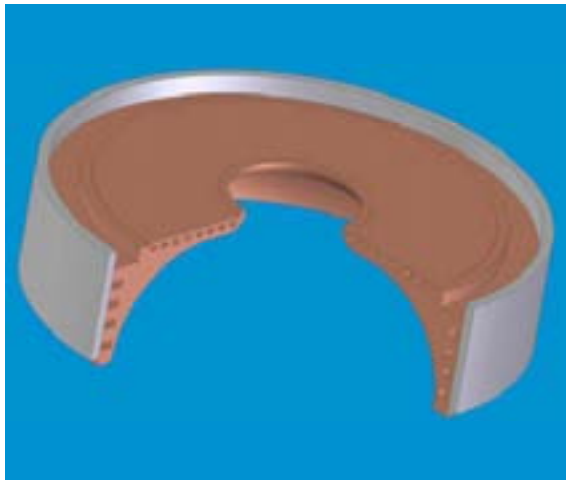


Structure Type	TW
Cell Number	50
Aperture 2a	60 - 46 mm
Attenuation τ	0.65
Q	22396 - 20562
Group velocity V_g/c	0.91% – 0.16%
Shunt impedance r	36.98 – 36.04 MΩ/m
Filling time T_f	3.44 μs
Power Dissipation	7.2 kW/m
E_0 (10 MW input)	7.3 MV/m

Pair of 2.2 m long $3\pi/4$ Mode TW Structures

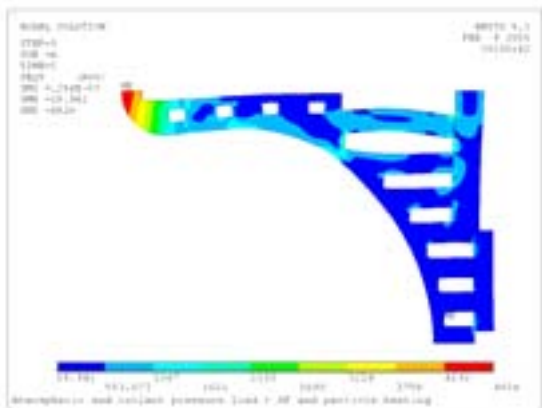
The regular 4.3 meter-long structure can be cut in half to form two 2.2 meter structures driven in series, permitting a triplet or quad doublet every 2.5 meters.



Thermal Simulation
for Regular Cells of SW Structure

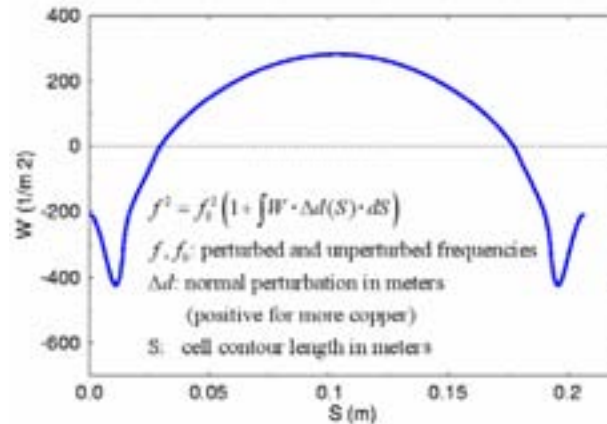
Design of Cooling Channels.

ANSYS thermal model with average RF losses (left) and thermal model with average RF and particle losses (right).



Deformation calculated from ANSYS

Calculation of Frequency Detuning due to Heating



Frequency Perturbation calculation based on weighting function and ANSYS results

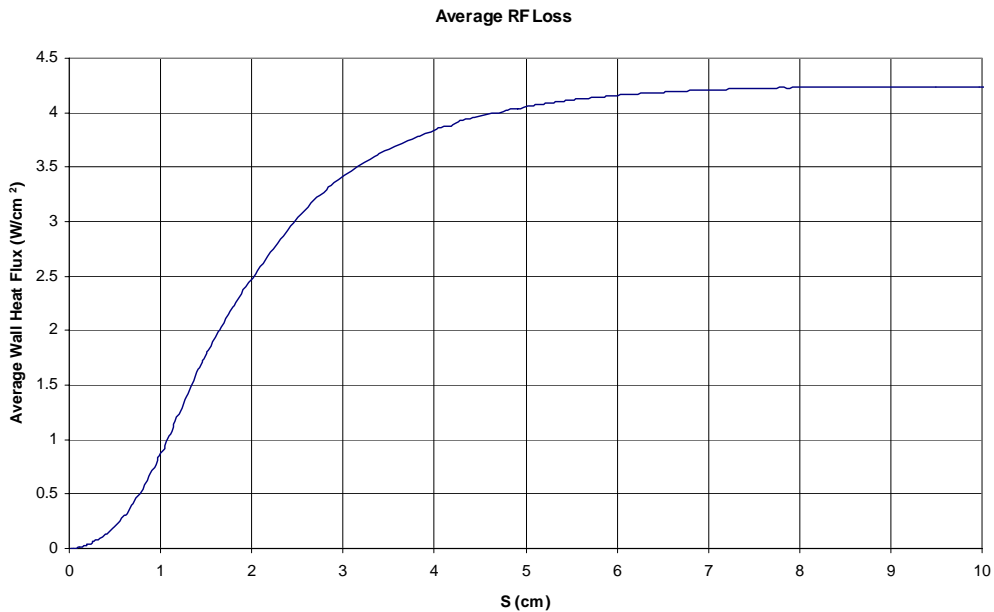
Case	Cavity detuning
Average RF losses only	-20.4 kHz
Average RF and particle losses	-58.6 kHz
Start of RF pulse, RF loss only	-19.5 kHz
End of RF pulse, RF loss only	-23.3 kHz
Transient detuning, RF only	-3.9 kHz
Start of RF pulse, RF and particle loss	-53.8 kHz
End of RF pulse, RF and particle loss	-68.9 kHz
Transient detuning, RF and particle loss	-15.1 kHz

* 6.5 m/s flow speed and 62.4 GPM / full cell



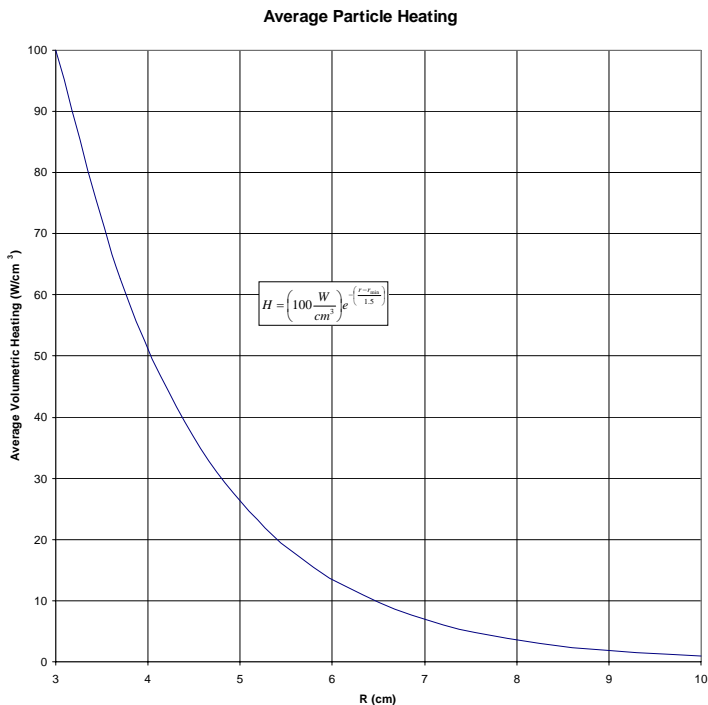
Heating from RF and Particle Losses

Average RF heating at 14.8 MV/m with
5 Hz, 1ms pulses.



3.5 kW / full cell

Average particle heating
For conventional source



6.8 kW/ full cell

Mode Spacing

For N coupled resonators:

$$\omega_q^2 = \frac{\omega_0^2}{1 + k \cos \frac{\pi q}{N}} \quad q = 0, 1, 2, \dots, N$$

The mode spacing between π and nearest mode is

$$\frac{\Delta\omega}{\omega} \approx \frac{k\pi^2}{4N^2}$$

For examples,

In our SW20PI structures built earlier, the spacing between π mode and $13\pi/14$ mode is 7 MHz,
 $6\pi/7$ mode is 28 MHz.

In L-Band 11-cell SW structure, coupling coefficient $k=0.0125$ and the spacing between
 π mode and $9\pi/10$ mode is 0.4 MHz,
 $4\pi/5$ mode is 1.6 MHz.

Cell Phase Difference - I

There are phase differences along structure due to the RF feed and loss along the structure.

The phase difference between neighbor cells is

$$\Phi_n - \Phi_{n-1} = \frac{\sqrt{1-k}}{kQ} [2(N-1) + 1]$$

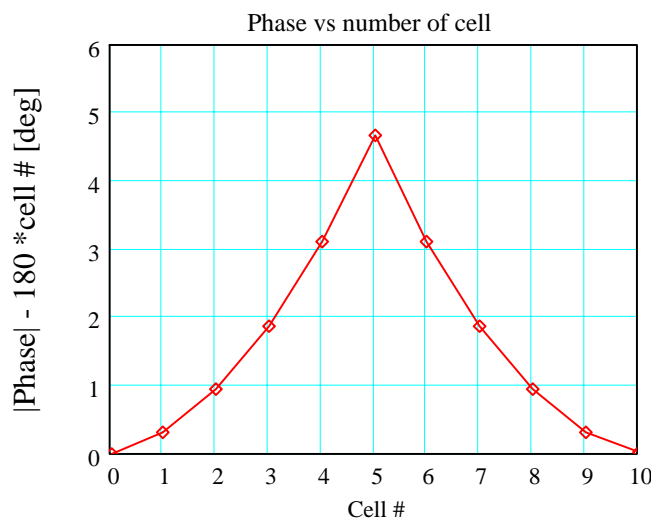
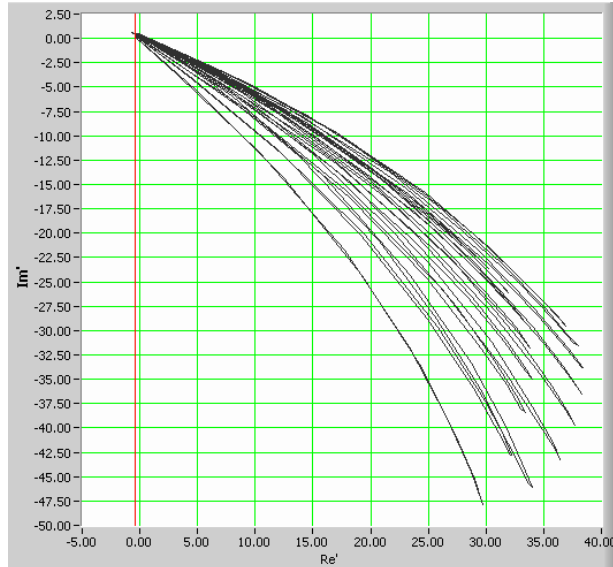
Linear increasing towards driving cell

The total phase difference is

$$\Delta\Phi = \frac{\sqrt{1-k}}{kQ} n^2$$

Total phase change
~ square of cell number
counting from driving cell

Cell Phase Difference II



In our SW20PI 15-cell SW structures, the S11 was measured while a small bead puling through the structure, the vector was plotted as shown.

Calculation: $\Delta\Phi \sim 6.2^\circ$

Measurement $\Delta\Phi \sim 7.5^\circ$

For 11-cell L-Band structure,
The calculated $\Delta\Phi \sim 3.8^\circ$.

Equivalent circuit simulation: $\Delta\Phi \sim 4.6^\circ$,
($\cos 4.6^\circ = 0.997$ – negligible influence).

Power Reflection and Phase Change due to Frequency Deviation

Reflected coefficient:

$$\Gamma = -1 + \frac{2\beta}{\beta + 1 + j \frac{2Q_0\Delta f}{f}}$$

Phase shifting:

$$\Phi = \text{Arg}(\Gamma + 1) = \tan^{-1} \frac{2Q_0\Delta f}{f(\beta + 1)}$$

For an example, at $\beta=1$ case:

$$\Gamma = -1 + \frac{1}{1 + j \frac{Q_0\Delta f}{f}}$$

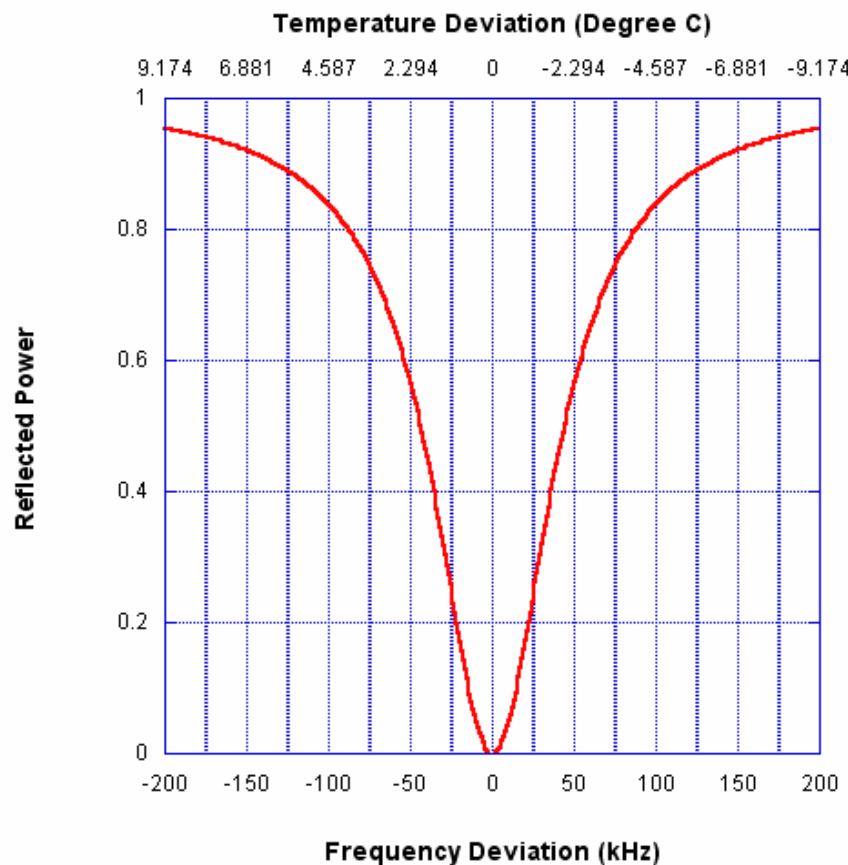
$$\Phi = \tan^{-1} \frac{Q_0\Delta f}{f}$$

For present cooling design for capture section with large particle loss, the transient Δf due to 1 ms RF pulses is 15.0 kHz (0.69° C), correspondingly, $\Gamma^2 \sim 0.1$ and $\Delta\Phi \sim 18^\circ$.

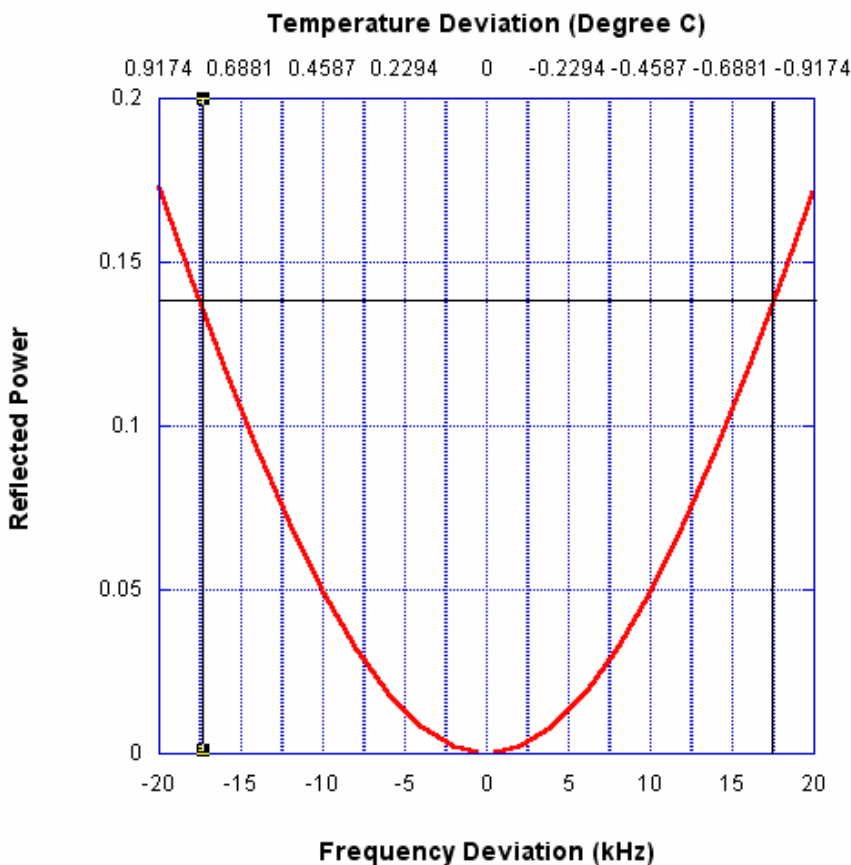
- The operation temperature can be optimized.
- The transient temperatures change can be further reduced.
- No problem in water temperature stabilization.
-- experience for SLC accelerator structures

Power Reflection due to Frequency Deviation

Reflected Power as Functions
of Frequency & Temperature Deviation ($\beta=1$)

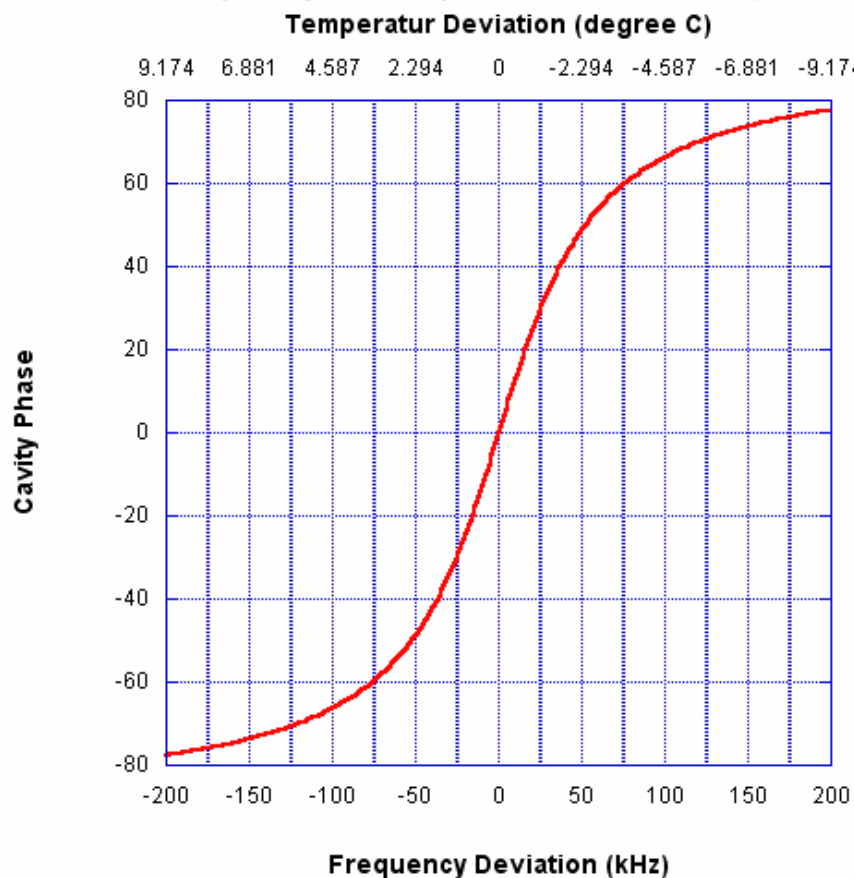


Reflected Power as Functions
of Frequency & Temperature Deviation ($\beta=1$)

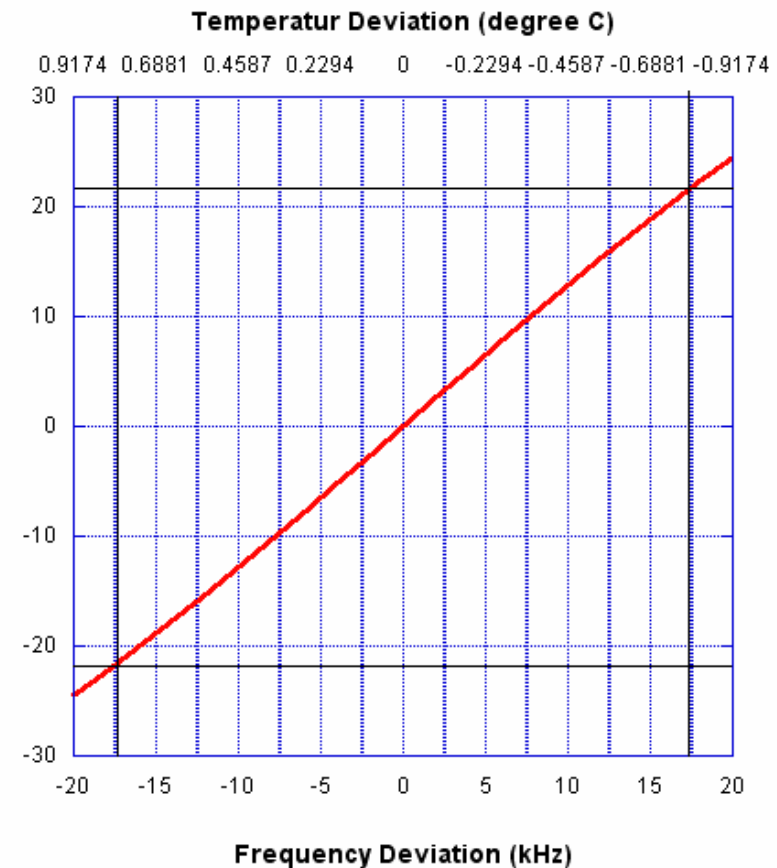


Phase Change due to Frequency Deviation

Cavity Phase as Functions
of Frequency & Temperature Deviation (beta=1)



Cavity Phase as Functions
of Frequency & Temperature Deviation (beta=1)





Field Amplitude Change due to Frequency Deviation

From the perturbation solution for a resonator chain matrix,
the effect to amplitude due to detuning errors:

$$\frac{\delta X^\pi(n)}{X^\pi(n)} = \sum_{p=1}^N \frac{\tilde{\varepsilon}_p (1-k) \cos \pi \frac{pn}{N}}{k(1-\cos \pi \frac{pn}{N})}$$

where $\tilde{\varepsilon}_p$ is Fourier transform of
the error distribution

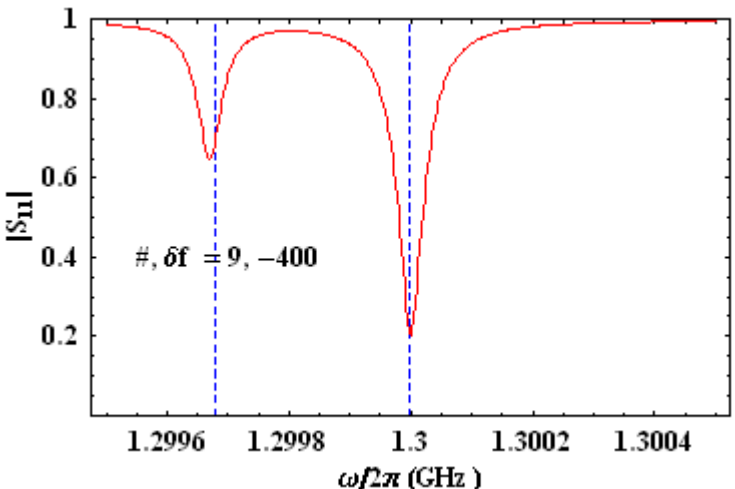
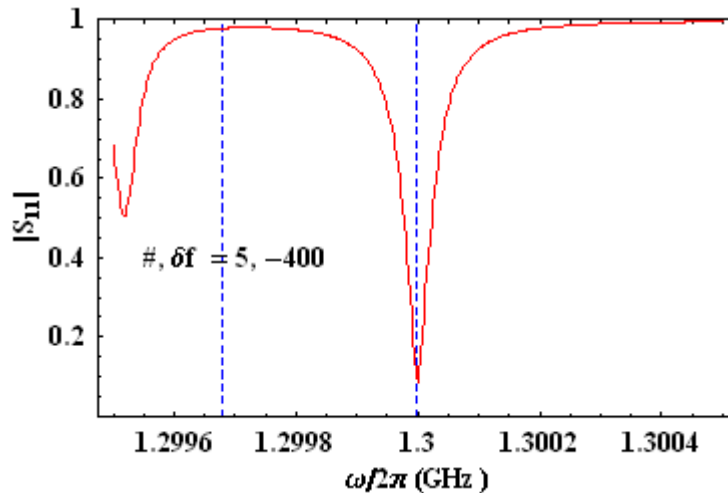
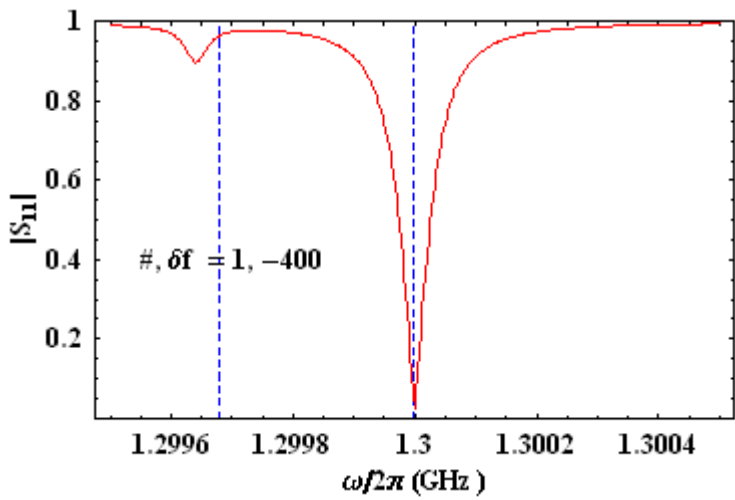
$$\tilde{\varepsilon}_p = \frac{2}{N} \sum_{r=0}^N W(p) \frac{\delta \omega_{0r}^2}{\omega_{0r}^2} \cos\left(\frac{\pi pr}{N}\right)$$

$$\dot{\omega}_{0r}^2 = \omega_{0r}^2 + \delta \omega_{0r}^2 \quad \begin{array}{l} W(n)=1, n=1, \dots, N \\ W(n)=1/2, n=0, N \end{array}$$

Simply to estimate for the simplest and worst case of $\Delta f \sim 17$ kHz,
the average amplitude change $\sim 5.0\%$.

- No problem for tuning accuracy from the X-Band experiences and transient temperature fluctuation.

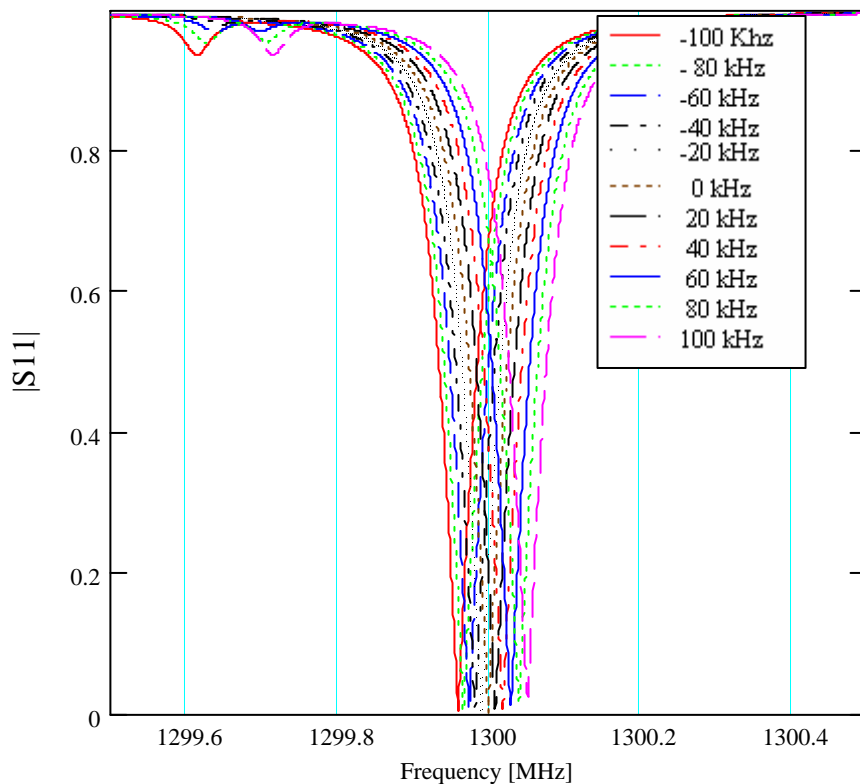
S_{11} Change due to Cell Frequency Deviation



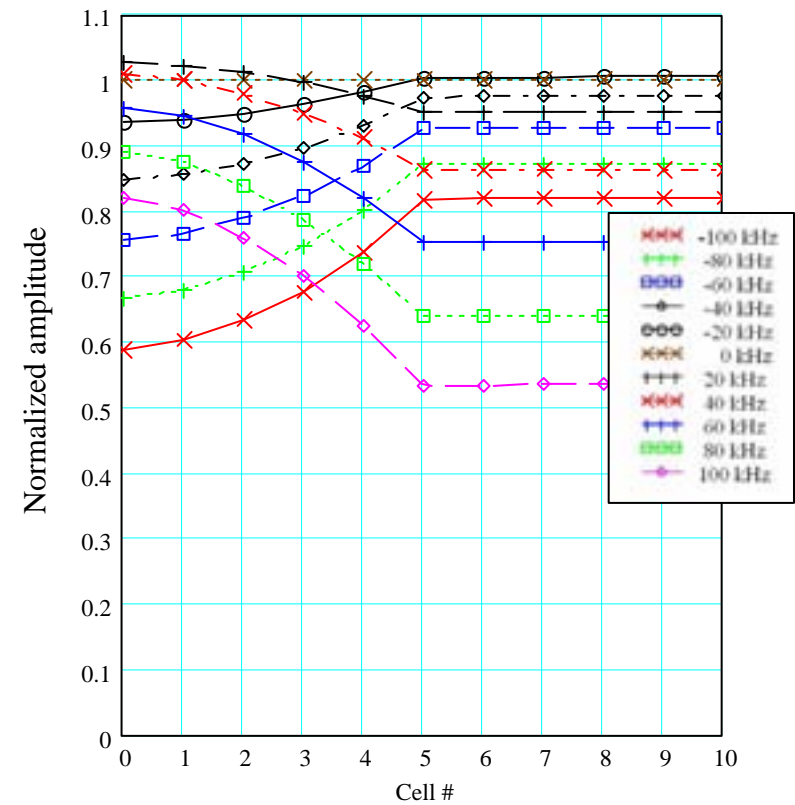
The cell number #1, #5, #9 and frequency change ± 400 kHz are shown in each figure.

S₁₁ Field Amplitude Change due to Frequency Deviation

Shifting frequency of first five cells



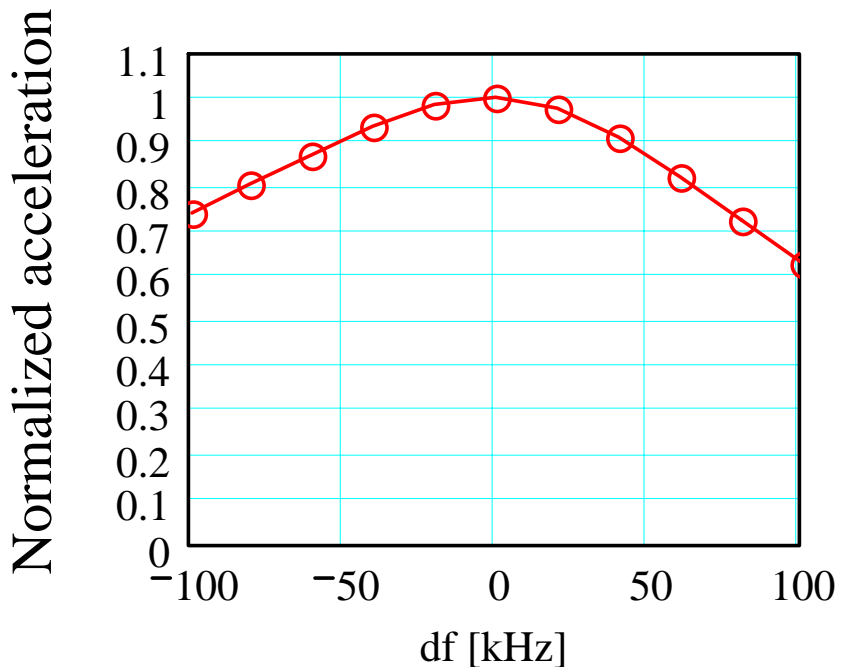
S₁₁ vs. frequency



Field profile

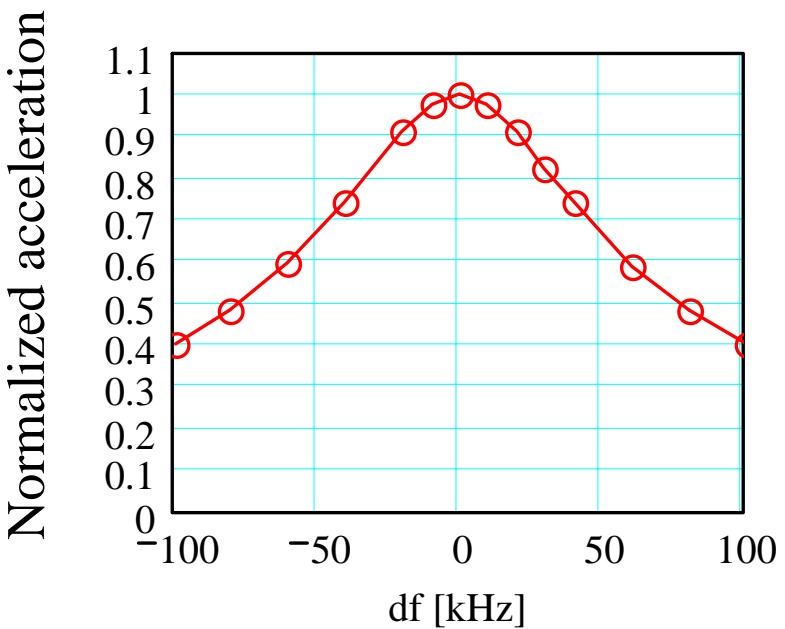
Total Acceleration Change due to Frequency Deviation

Shifting frequency of first five cells



Change of acceleration for fixed power,
fixed frequency and optimal phase shift.

Shifting frequency of every cell

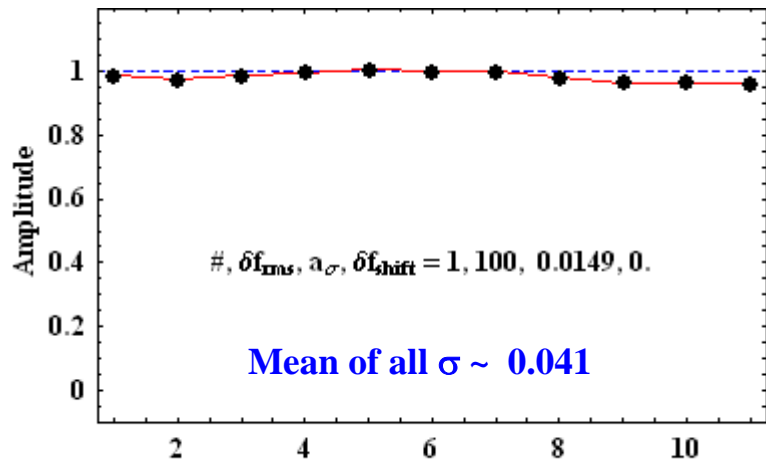


Change of acceleration for fixed
power, fixed frequency and optimal
phase shift.

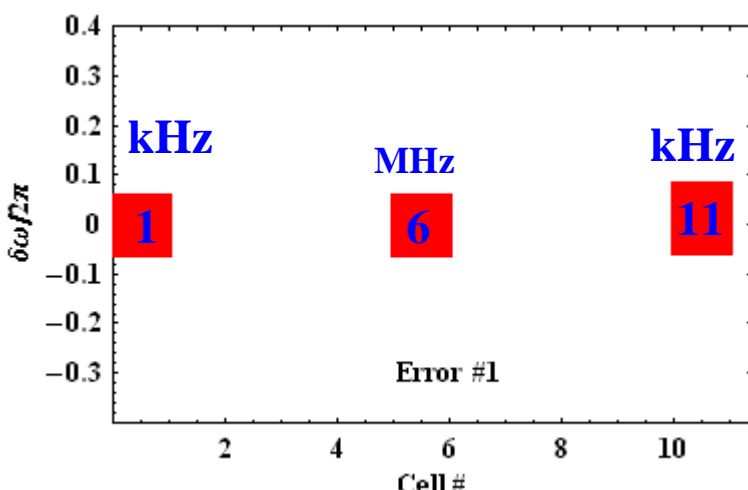


Field Amplitude Change

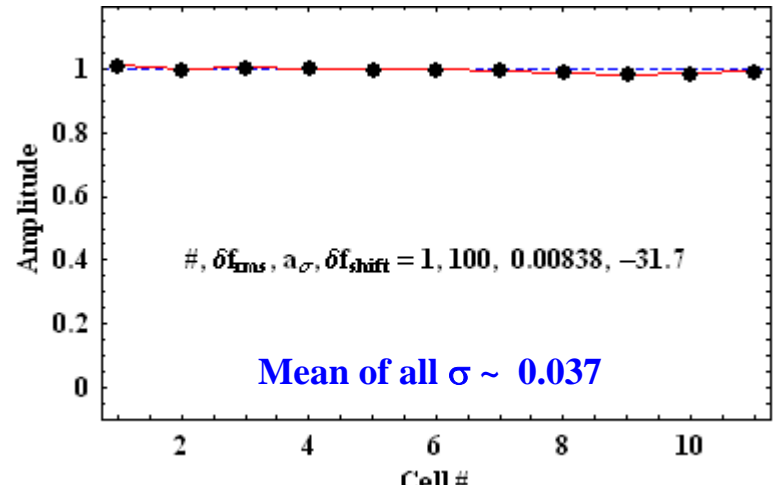
for RMS 40 kHz Random Cell-To-Cell Errors



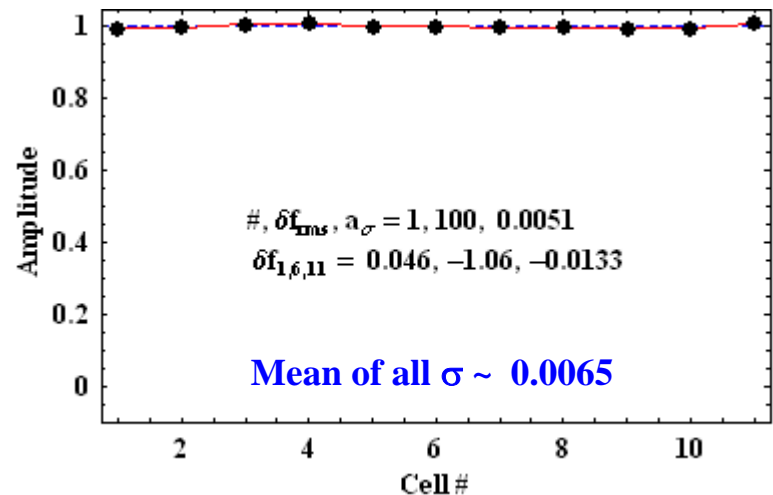
No corrections are made



The first, middle and last cell are tuned together with a systematic shift in the cell freqs,



A systematic shift is made in the all of the cell freqs (tuning via water cooling),



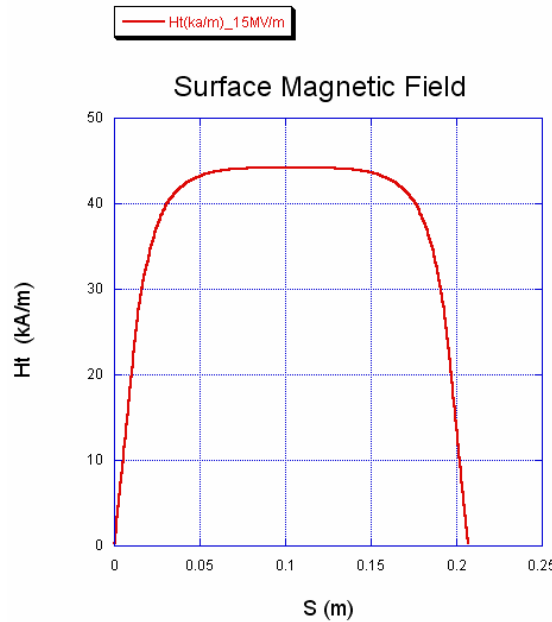
Mean of all $\sigma \sim 0.0065$

Freq tuning required of the three cells

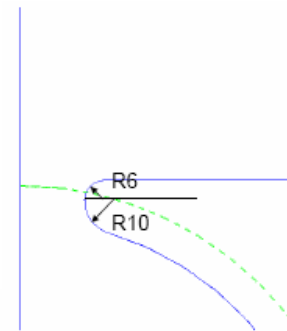
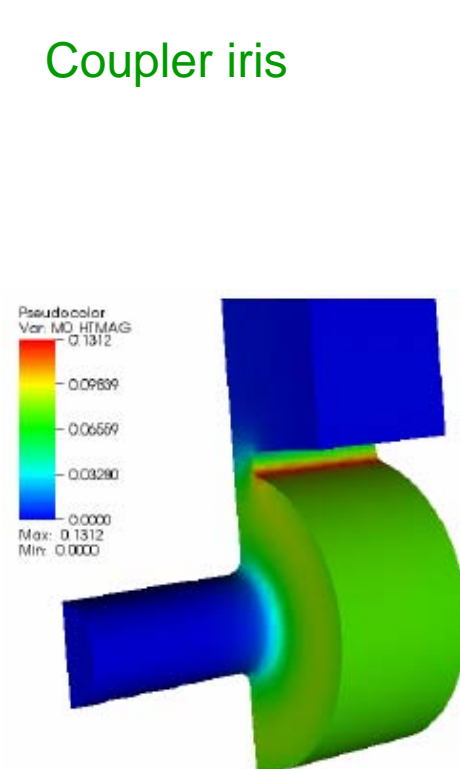
RF Pulse Heating

$$\Delta T = H_t^2 \sqrt{T_p} \frac{R_s}{\sqrt{\pi \rho c \kappa}}$$

Regular cell



Coupler iris



$E_{\text{acc}} = 15 \text{ MV/m}$
 $T_{\text{pulse}} = 1.0 \text{ ms}$
 $H_{S,\text{max}} = 67 \text{ kA/m}$
 $\Delta T = 21 \text{ }^{\circ}\text{C}$

The maximum H_t along cell profile
is 43.8 kA/m for $E_a=15$ MV/m.

The maximum ΔT is $\sim 8.5^{\circ}\text{C}$ in the outer wall.



The principle of Initial Deceleration Scheme

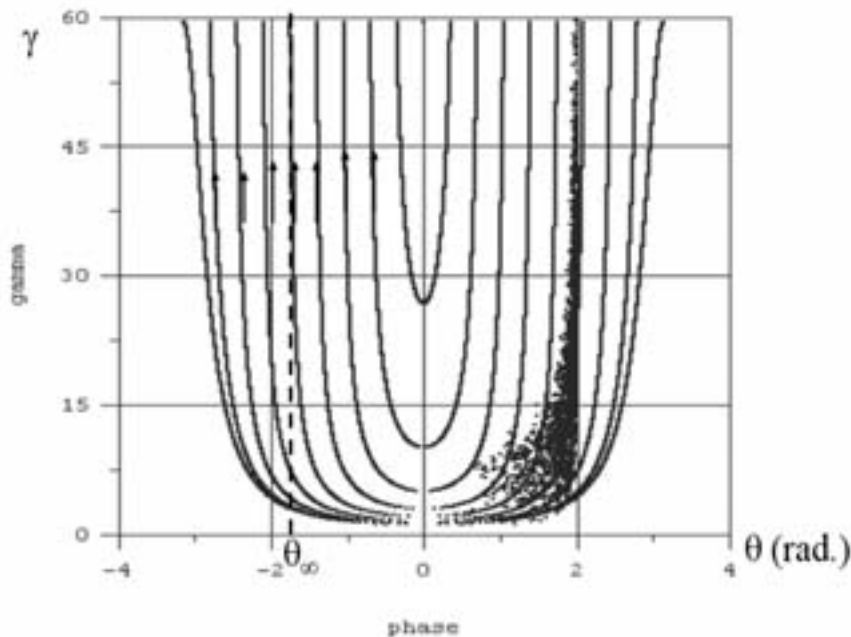
In a phase velocity $V_p=c$ TW structure, the equation for the particle orbit in phase space is

$$\cos \theta - \cos \theta_{\infty} = \frac{2\pi m_0 c^2}{eE_0 \lambda} \left[\sqrt{p^2 + 1} - p \right] = \frac{2\pi m_0 c^2}{eE_0 \lambda} \sqrt{\frac{1 - \beta_e}{1 + \beta_e}}$$

Where E_0 is accelerating gradient and p is normalized momentum expressed by

$$p = \gamma \beta_e = \sqrt{\gamma^2 - 1}$$

The approach is initially decelerating the positrons and arranging the phase and amplitude of the fields so that the distribution in longitudinal phase space of the incoming positrons lay along one of the orbits in longitudinal phase space. Thus the positrons approached a small spread in asymptotic phase as their energy increased.



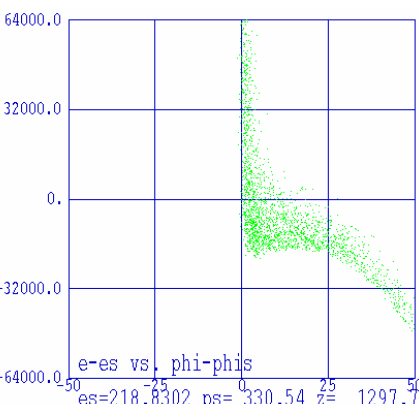
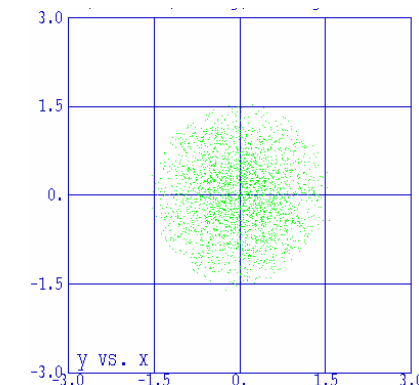
Longitudinal phase space of positrons from target in a phase velocity $V_p=C$ TW structure



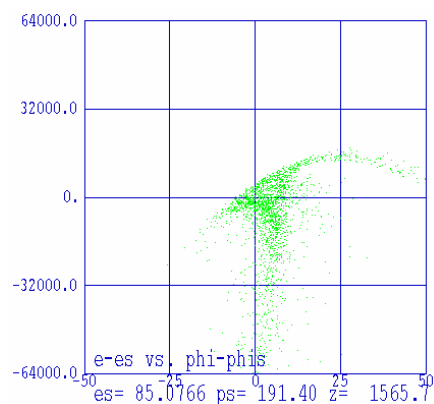
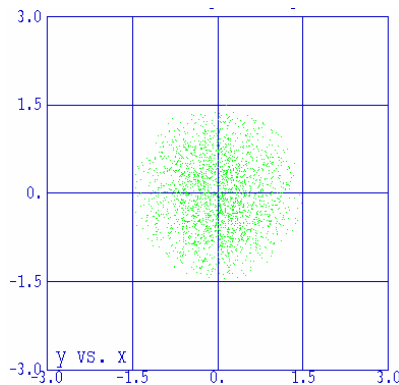
Increase of Positron Yield by Initial Deceleration

PARMELA Simulation:

Superconducting coils with optimized tapered magnetic field,
13299 e+ from shower in target,
TW wave, acceleration with 15 MV/m and deceleration with 5.5 MV/m,
Collimated in aperture for 0.03 m-rad emittance without bunch compression,
Collimated in phase and energy for 1% and 2% spectra.



Initial Acceleration Case



Initial Deceleration Case

Deceleration Yields

1% spectrum: 1.47 e⁺/e⁻
2% spectrum: 1.84 e⁺/e⁻

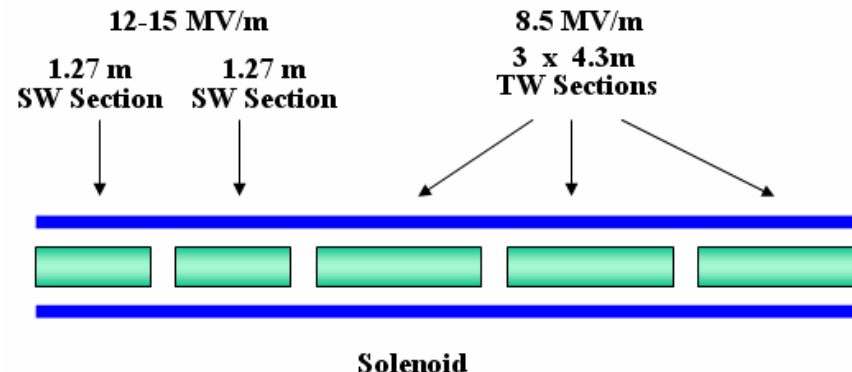
Acceleration Yields

1% spectrum: 1.01
2% spectrum: 1.27

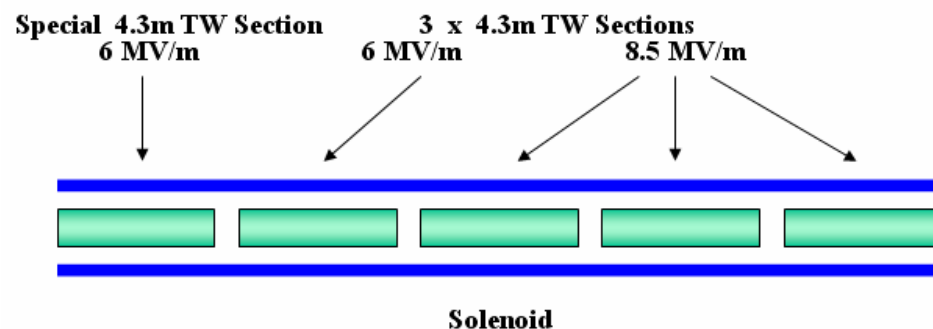
Yields with initial deceleration are
about 40% higher than with initial
acceleration

Capture Region for Conventional Positron Source

Layout of the capture region for conventional positron source in the acceleration scheme.



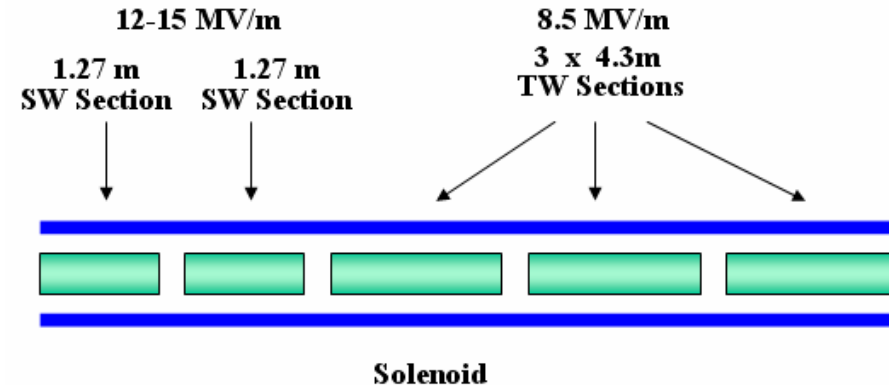
Layout of the capture region for conventional positron source in the scheme with initial deceleration.



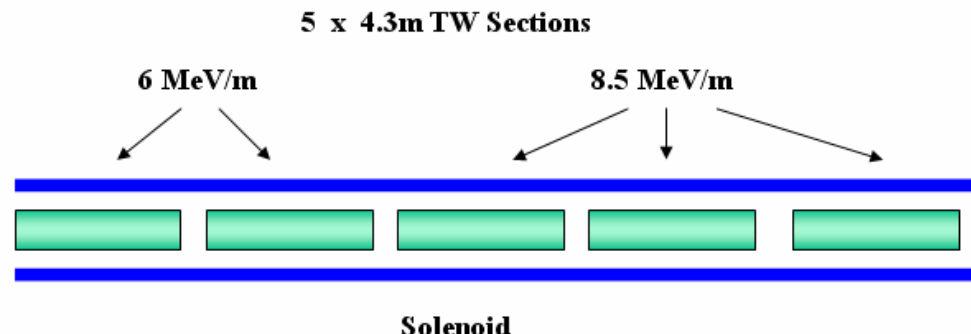


Capture Region for Undulator Based Positron Source

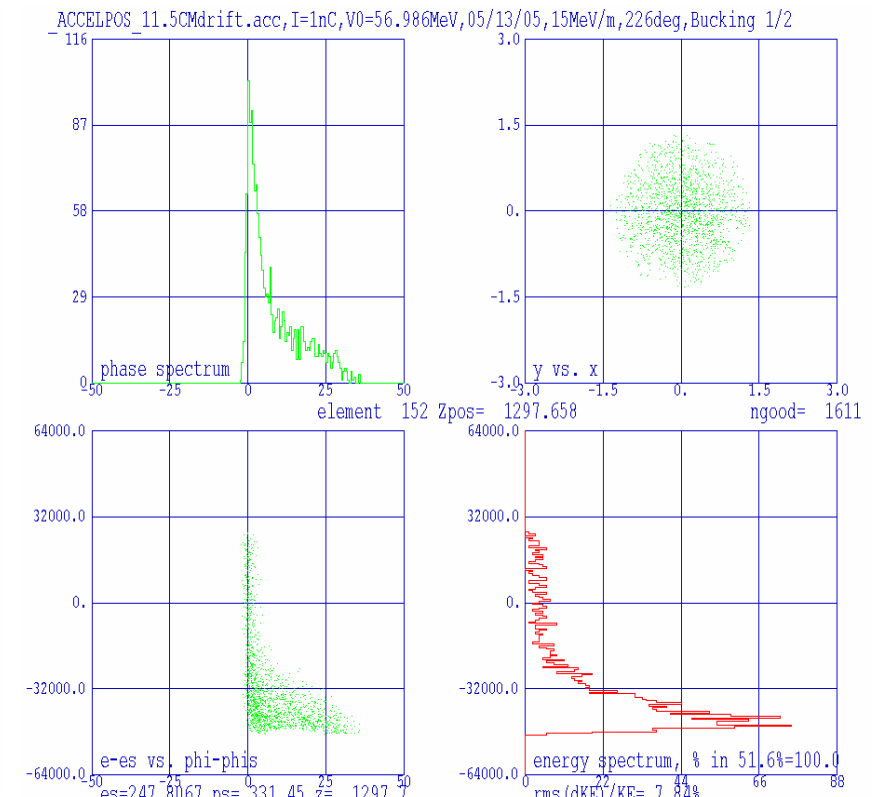
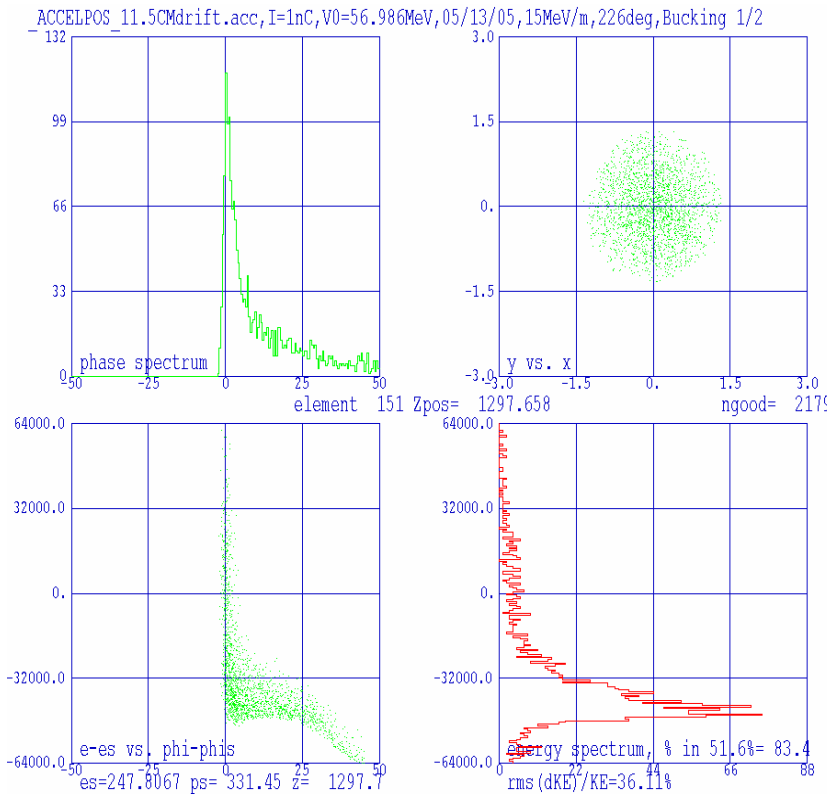
Layout of the capture region for undulator based positron source in the acceleration scheme.



Layout of the capture region for undulator-based positron source in the scheme if initial deceleration.

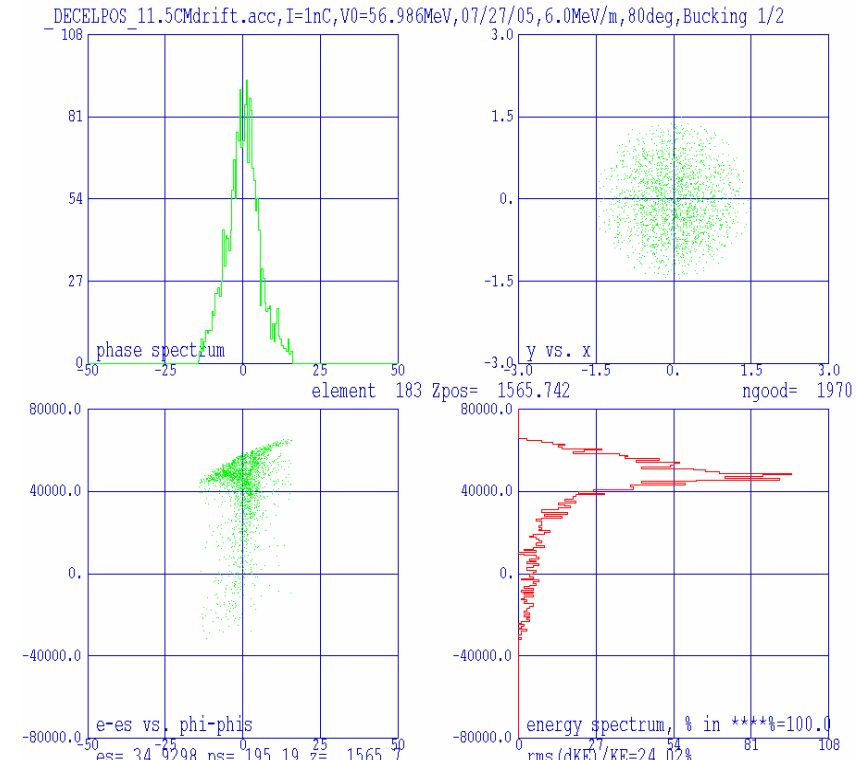
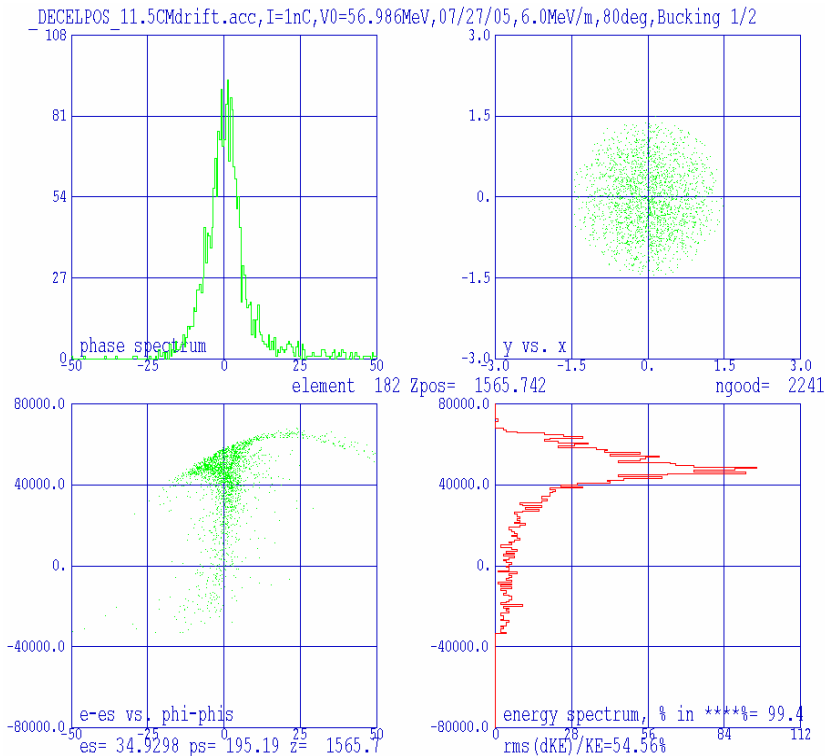


Positron Capture Simulation with Initial Acceleration



PARAMELA simulation of the positron capture for the case of initial acceleration.
The right four plots show the acceptable positrons by the damping ring.

Positron Capture Simulation with Initial Deceleration



PARMELA simulation of the positron capture for case of initial deceleration.
The right four plots show the acceptable positrons by the damping ring.
Yield of two can be obtained for 30 degrees phase and 2% spectrum.



Plan for Test Structures

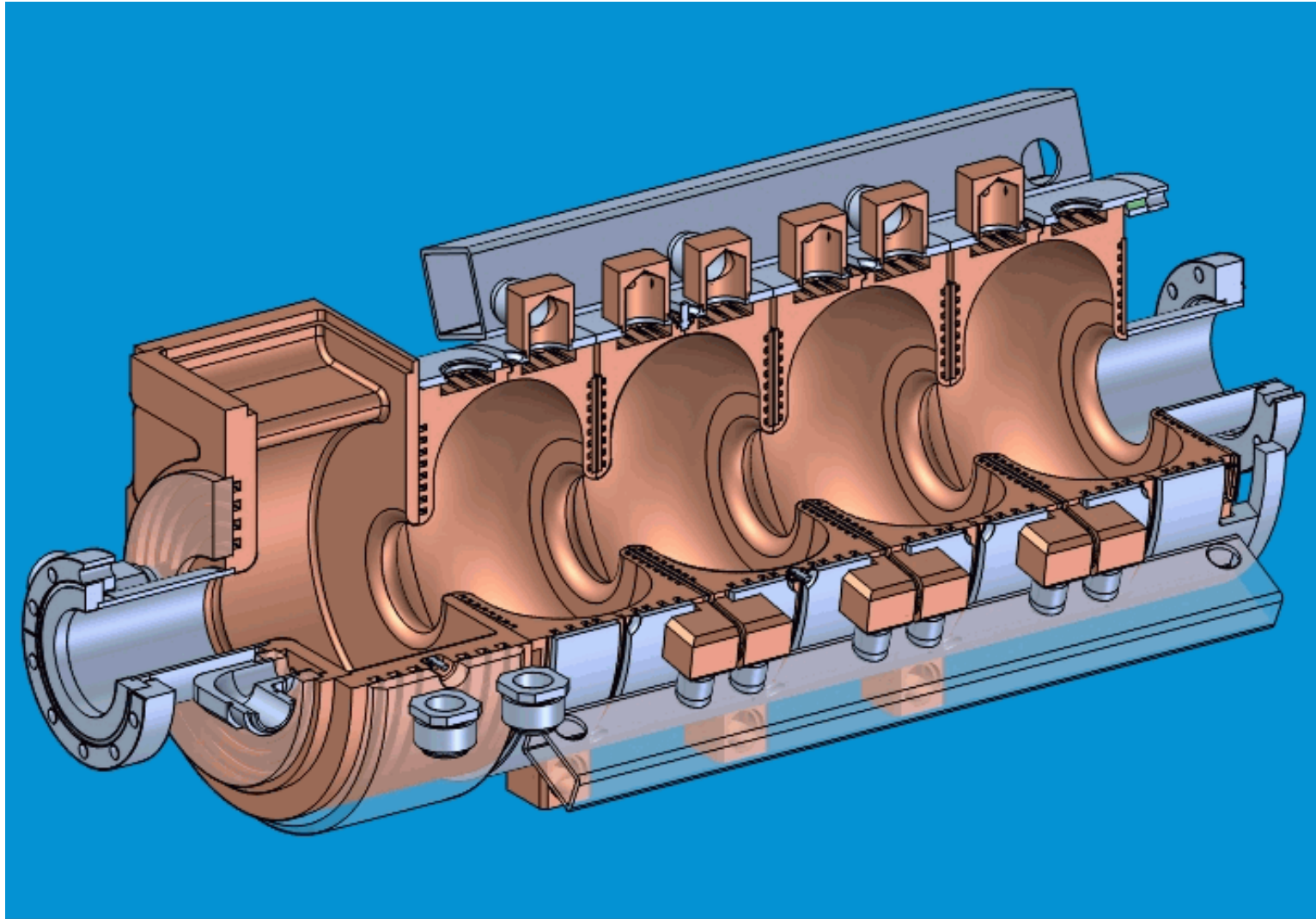
Based on our preliminary studies, we have concluded the merit and feasibility of structures design for the PPS. We plan to start with the fabrication and test of a short 5-cell SW test section.

TH2095A or TH2104U klystron
5 MW peak power, 1 ms, 5 Hz.

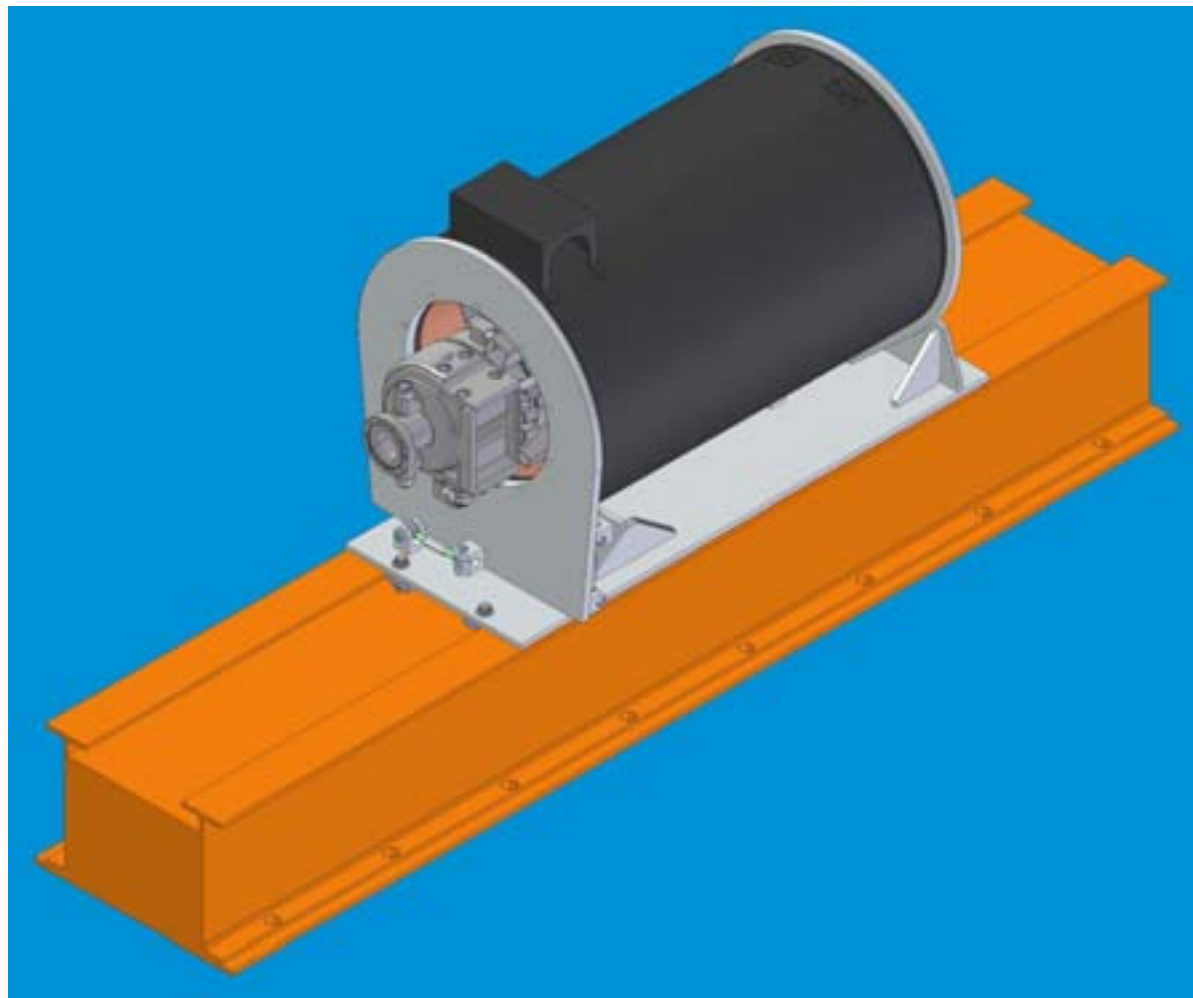
Cell Number	5
Aperture 2a	60 mm
Disk thickness	18 mm
Q	29700
Shunt impedance r	34.3 MΩ/m
Power needed at 15 MV/m	3.8 MW
RF Pd at 15 MV/m	3.6 kW/cell
Particle Pd	6.8 kW/cell
ΔT (Average/Transient) °C	2.0 / 0.69



5-Cell Test SW Structure

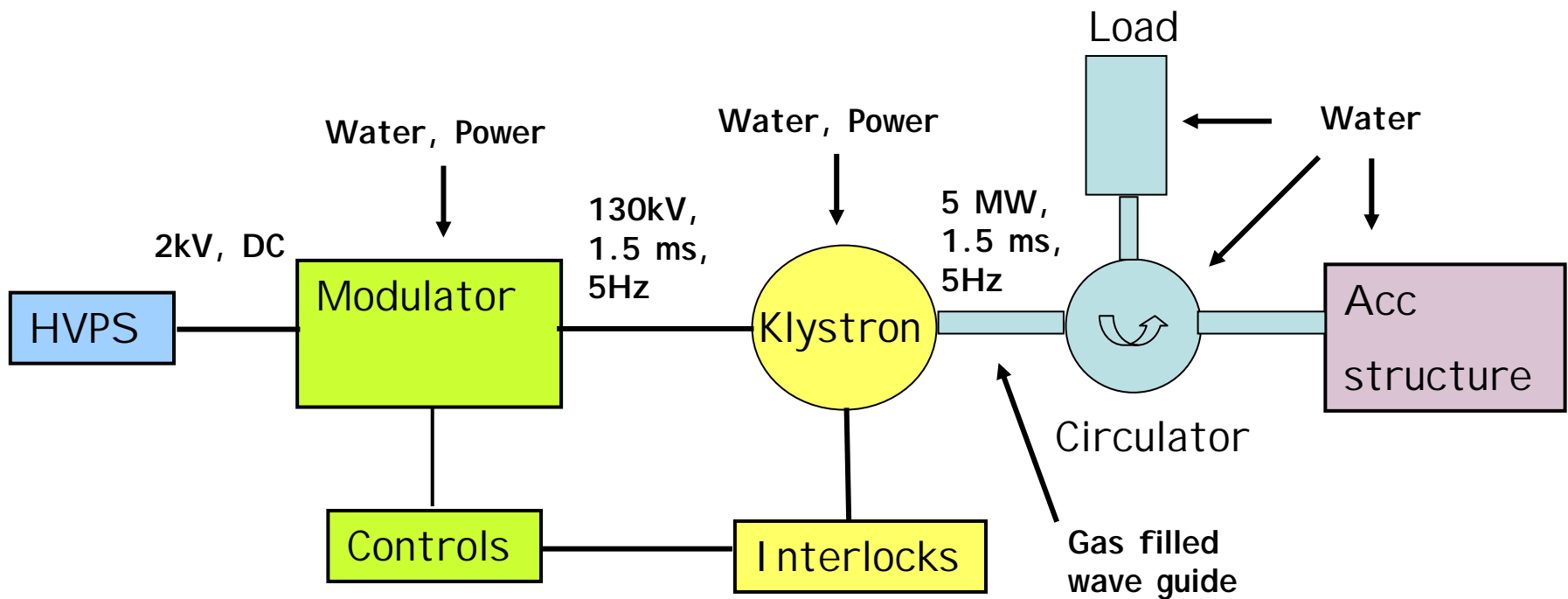


Installation of Test SW Structure



First test SW structure with a solenoid (used for 2104U and 2104C klystrons) on a girder.

L-band Test Stand in End-station B at SLAC



12/2005

1/2006

6/2006

Summary

1. We have a baseline design – minimum or starting point.
2. More studies will be related to
 - Overall parameter adjustment of positron source,
 - Cost and feasibility,
 - Experimental results of test structures.
3. We would like to have your comments and input.